Hindawi
Advances in Materials Science and Engineering
Volume 2018, Article ID 7093978, 9 pages
https://doi.org/10.1155/2018/7093978

Research Article

Impact Analysis of Brake Pad Backplate Structure and Friction Lining Material on Disc-Brake Noise

Gongyu Pan and Lei Chen

School of Automotive and Traffic Engineering, Jiangsu University, Zhenjiang 212013, China

Correspondence should be addressed to Lei Chen; js_chenlei@126.com

Received 29 December 2017; Accepted 7 March 2018; Published 29 March 2018

Academic Editor: Rujie He

This study proposes a three-layer brake pad design, on which a six-DOF dynamic model of brake disc-brake pad is established, and the factors affecting the system instability are analyzed. The analysis shows that the change of mass and stiffness of the brake pad will affect the stability of the system. From the linear complex eigenvalue analysis, the unstable vibration modes of the brake system are predicted, and the effectiveness of the complex mode analysis model is verified by the brake system bench test. Brake pads with different structural shapes are designed, and their influence on the stability of the brake system is analyzed. The results show that the design of the three-layer structure and the slotting design of the brake pad can effectively reduce the occurrence of the brake squeal, especially that of the high-frequency squeal noise.

1. Introduction

Since the early 1920s, automotive disc-brake squeal noise has been a widespread concern of academics and automobile manufacturers all over the world because brake squeal is an important cause of customer dissatisfaction and warranty problems. In the past three decades, the proportion of disc brake used in sedan has increased year by year. It can be assumed that disc brakes will gradually replace drum brakes in sedan. However, the problem of brake noise of disc brakes still exists, and many brake noise phenomena have not been explained rationally so far [1–3]. Automobile braking process will produce vibration, and unstable vibration will not only lead to noise that both affects the comfort of driving and causes acoustic pollution to the surrounding environment but it will also cause fatigue wear on the automobile brake system [4].

Lars have slotted and surfaced the surface of the brake disc and proved by experiment that improved brake disc can reduce the occurrence of the brake squeal [5]. Oberst and Lai used chaos theory to study the mechanism of braking noise, which is of great guiding significance [6]. Kung et al. calculated the free modal of the components in the brake and obtained the components and related modalities with the largest contribution rate of unstable mode by the complex eigenvalue analysis [7]. In addition to using the complex eigenvalue analysis to study the brake noise, the transient dynamic analysis is first used by Nagy et al. The four mode frequencies extracted from the results of transient dynamic analysis coincide with the experimental noise [8]. The disadvantages of transient dynamics are that it takes too much computation time and takes up a lot of disk space, and it is also hard for the data to be used directly for design changes. Besides, because of the high frequency of brake squeal, the explicit integral time step is very small, whereas the implicit integral can have a large time step, but it will attenuate the high-frequency mode. Complex eigenvalue analysis and transient dynamic analysis are used by AbuBakar and Ouyang [9] to study the brake squeal, under the same model and boundary condition. The results of the above two analyses are identical with the different contact mechanism and integral method. In the analysis of

the brake system noise, the use of complex eigenvalue analysis, combined with a reasonable combination of transient dynamic analysis, may be a way to analyze the noise generation mechanism.

In the friction-slip experiment of the flat plate, Chen [3] found that the instantaneous squeal may not be caused by the modal coupling, and the transient excitation between the disc and block may be the key mechanism of the squeal. However, this kind of alternating load excitation is a transient process difficult to capture through experiments. The transient dynamic analysis may more clearly show the process and reveal the reasons of this phenomenon. For the dynamic model of the brake disc and brake pad, a four-DOF self-excited frictional oscillator model was proposed by Zhang et al. [10] to explore the difference between the linear analysis and nonlinear analysis on the brake system noise, and corresponding improvement measures are given.

In this context, based on the modal coupling theory, a six-degree-of-freedom motion model of the brake disc and brake pad is established. Combined with finite element complex modal analysis and bench test, it is of great guiding significance to improving the NVH performance by improving the material properties of the brake pad and optimizing the backplate structure of the brake pad to inhibit the brake squeal noise and to exploring the inhibition mechanism of noise, which provides a theoretical basis for reducing the noise of brake squeal.

2. Six-DOF Kinematics Model of Brake Disc-Brake Pad

The brake coupling model built by Festjens et al. [11] shows that the structure and damping of backplate of the brake pad have an important influence on the brake noise. Similarly, the damping size of the friction lining material will also have a significant influence on brake noise. Through the research studied by Ruhai et al. [12], it is known that adding a certain proportion of viscoelastic material to the friction lining could reduce the resonance tendency between the brake pad and the brake disc, thereby inhibiting the brake squeal to some extent. Based on the important influence of the friction lining, it is divided into two parts, namely, lining substrate and friction lining mixture. Since the material composition of lining substrate has stronger damping characteristics than the friction lining mixture, it should be treated differently during the modeling and simulating process.

A six-DOF kinematics model of brake disc-brake pad is depicted in Figure 1. Due to the small damping of the system, the effect of damping is neglected in the kinematics analysis. The brake pad is composed of the brake pad backplate m_b, lining substrate m_u, and friction lining mixture m_l. m_b has a z-direction degree of freedom z_1; m_u has a z-direction degree of freedom z_2; and m_l has a z-direction degree of freedom z_3 and an x-direction degree of freedom x_3; The brake disc m_d has two degrees of freedom, respectively, x-direction of x_d and z-direction of z_d. μ, P, and N are friction coefficient, force of piston acting on the brake pad, and positive force acting on the brake disc, respectively.

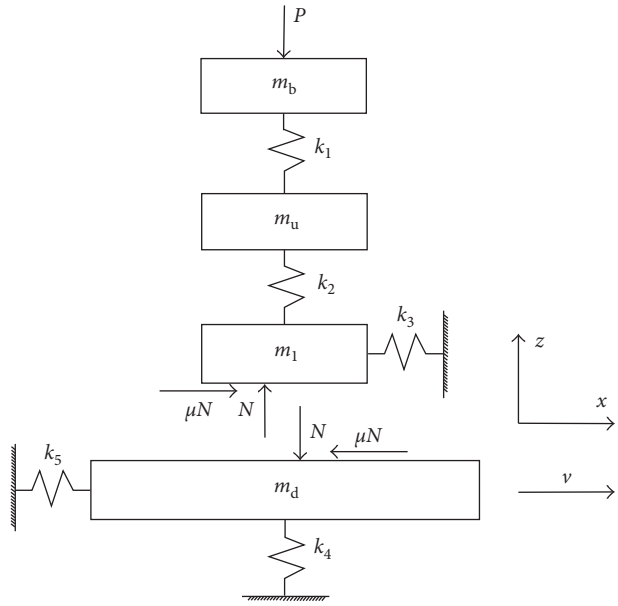

Figure 1: Six-DOF kinematics model of brake disc-brake pad.

The kinematic equation can be obtained from the kinematic model of Figure 1:

$$[M]\{\ddot{u}\} + [K]\{u\} = \{F\}. \tag{1}$$

In this formula, $u = (z_1, z_2, z_3, x_3, z_d, x_d)^T$ and $(\cdot)$ is the differentiation with respect to time. The mass matrix $[M] = \mathrm{diag}(m_b, m_u, m_l, m_l, m_d, m_d)$, motivation $\{F\} = (P, 0, N, \mu N, -N, -\mu N)^T$, and $[K]$ is the stiffness matrix:

$$[K] = \begin{bmatrix} k_1 & -k_1 & 0 & 0 & 0 & 0 \\ -k_1 & k_1 + k_2 & -k_2 & 0 & 0 & 0 \\ 0 & -k_2 & k_2 & 0 & 0 & 0 \\ 0 & 0 & 0 & k_3 & 0 & 0 \\ 0 & 0 & 0 & 0 & k_4 & 0 \\ 0 & 0 & 0 & 0 & 0 & k_5 \end{bmatrix}. \tag{2}$$

In the initial stage, the system is in a stable steady state, the brake disc rotates at a constant speed, and the system does not produce vibration, so the steady-state equation can be obtained. Assuming that the brake disc and brake pad are not separated during the process of vibration, the constraint condition is $z_d = z_3$, and then we know

$$N = m_l\ddot{z}_3 - (k_1 + k_2)z_1 + k_2 z_2. \tag{3}$$

Taking (3) into the steady-state equation, we obtain

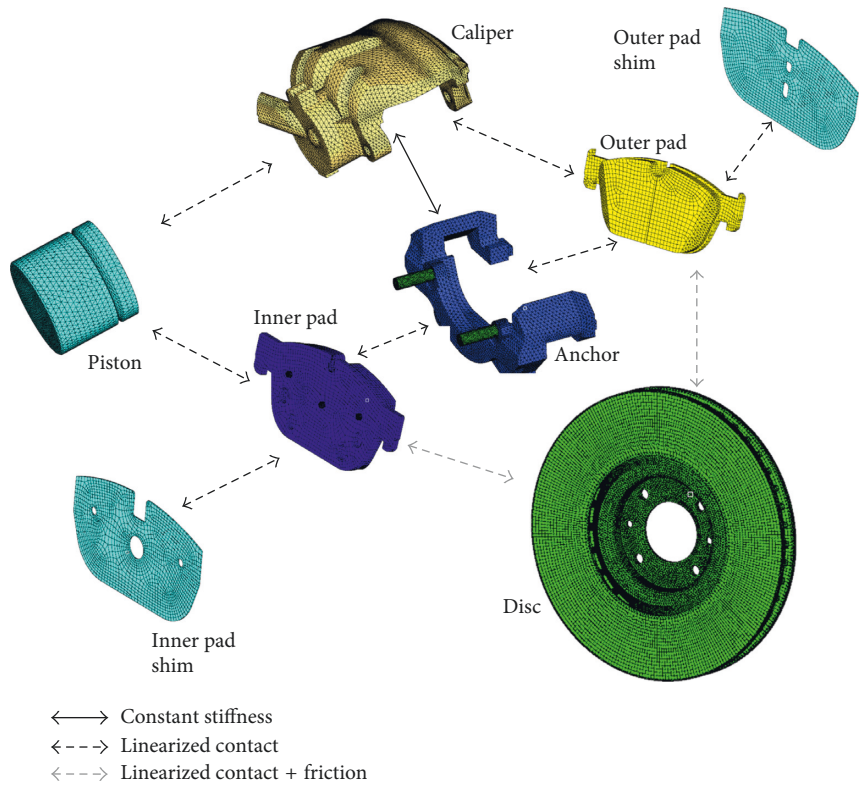

Figure 2: Finite element model of brake.

$$\begin{bmatrix} m_b & 0 & 0 & 0 & 0 \\ 0 & m_u & 0 & 0 & 0 \\ 0 & 0 & m_l + m_d & 0 & 0 \\ 0 & 0 & -\mu m_l & m_l & 0 \\ 0 & 0 & \mu m_l & 0 & m_d \end{bmatrix} \cdot \begin{Bmatrix} \ddot{z}_1 \\ \ddot{z}_2 \\ \ddot{z}_3 \\ \ddot{x}_3 \\ \ddot{x}_d \end{Bmatrix} + \begin{bmatrix} k_1 & -k_1 & 0 & 0 & 0 \\ -k_1 & k_1 + k_2 & -k_2 & 0 & 0 \\ 0 & -k_2 & k_2 + k_4 & 0 & 0 \\ \mu(k_1 + k_2) & -\mu k_2 & 0 & k_3 & 0 \\ -\mu(k_1 + k_2) & \mu k_2 & 0 & 0 & k_5 \end{bmatrix} \cdot \begin{Bmatrix} z_1 \\ z_2 \\ z_3 \\ x_3 \\ x_d \end{Bmatrix} = \begin{Bmatrix} 0 \\ 0 \\ 0 \\ 0 \\ 0 \end{Bmatrix}. \tag{4}$$

Equation (4) is the kinematic equation of the brake disc-brake pad system. It can be found that the mass matrix and the stiffness matrix of the kinematic equation of system are both asymmetric due to the existence of friction, so the eigenvalues of the system may be complex numbers. The eigenvalues of the system can be obtained by complex modal analysis, where the imaginary part of eigenvalue represents the modal frequency and the real part represents the tendency of instability. At the same time, it can be found that the change of friction coefficient and the change of mass and stiffness of the brake pad will lead to the change of system mass matrix and the stiffness matrix, so as to change the system eigenvalue and affect the stability of the system. Based on the above, this study will change the system's mass matrix and stiffness matrix by changing the geometric characteristics of the brake pad backplate, thus affecting the stability tendency of the system, to find out which structural feature of the backplate can reduce the brake system squeal.

3. Numerical Model

3.1. Model of Complex Modal Analysis of Brake

3.1.1. Finite Element Model. Using CATIA to model the braking system, the HyperMesh is used to establish the mesh models, as shown in Figure 2. Among them, the brake caliper adopts the tetrahedral mesh (C3D4) due to the irregular structure, the remaining parts mainly adopt hexahedral unit (C3D8), supplemented with pentahedron unit (C3D6) and terahedral unit (C3D4), and the total number of model units is 327,568. Besides, the contact relationship between the components has been labelled in Figure 2.

3.1.2. Defining Material Properties. Define the material properties of each component, including Density, Young's modulus, and Poisson's ratio, as shown in Table 1.

3.1.3. Setting of Analysis. The finite element model, which has defined the material properties and assembled, is introduced into the ANSYS for complex eigenvalue analysis. Some nonlinear perturbation modal analysis is used to extract the unstable modes of the brake system.

Table 1: Material properties of brake components.

Component	Density (kg·m^{-3})	Young's modulus (MPa)	Poisson's ratio
Disc	7,190	122,000	0.230
Caliper	7,000	143,000	0.270
Backplate	7,800	197,000	0.300
Lining	2,615	8,600	0.330
Piston	7,220	180,000	0.300
Anchor	7,000	101,400	0.256
Guide pins	7,800	182,000	0.300

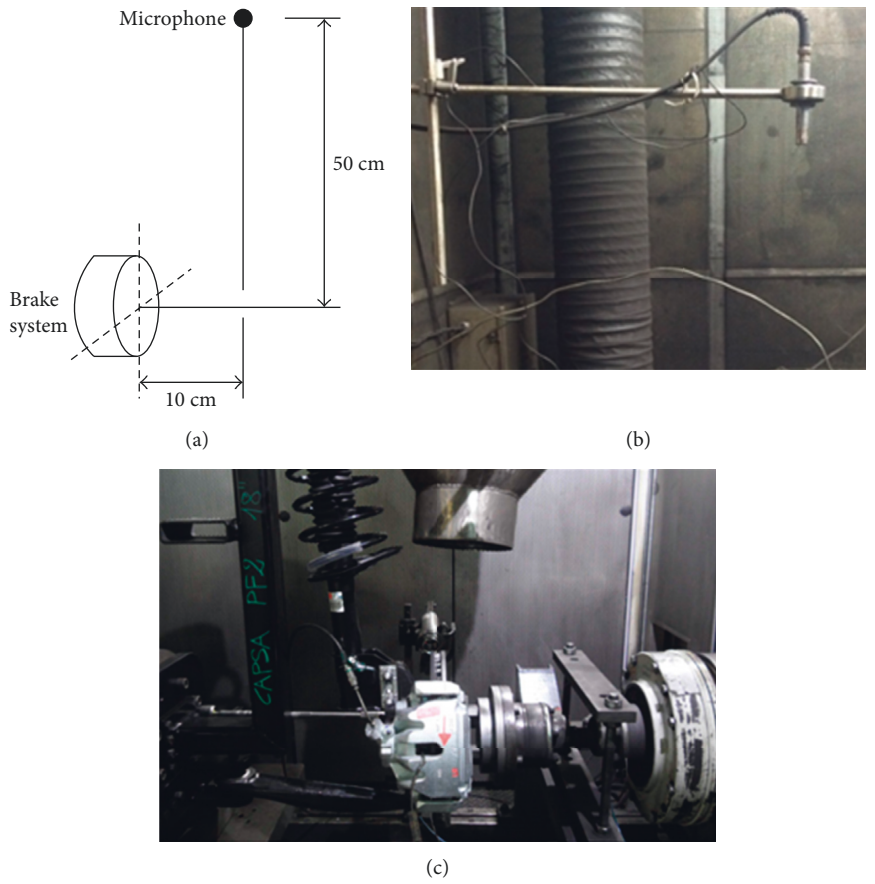

Figure 3: (a, b) Location of microphone and picture of real product and (c) disc brake assembled on test bench.

3.1.4. Settings of Boundary Conditions. The brake disc cap portion is bolted to the hub, but the brake disc can rotate along the z-axis, thus restraining the five degrees of freedom of the disc cap portion except for the z-direction of rotation. The anchor is bolted to the frame to restrain the six degrees of freedom of the cage bolt hole.

3.1.5. Setting of Load. In order to quantitatively study the relationship between friction coefficient, braking pressure, and brake noise, a brake system test was carried out under 9 operating conditions: by speed: 60 rpm, 120 rpm, and 180 rpm, and by hydraulic pressure: 1.5 MPa, 2.0 MPa, and 2.5 MPa.

3.2. Bench Test Verification of Brake Complex Modal Analysis Model. The test standard of brake noise is the NVH test standard of the Society of Automotive Engineers, namely, SAE J2521 test standard [13]; the microphone is placed at 10 cm in the horizontal direction of the brake system, and the vertical distance is 50 cm (Figures 3(a)and 3(b)).

In the whole experimental process, 18 stages of braking conditions of the noise test were measured and the total braking process was 1,430 times. Since the initial temperature of this test starts from zero, there is no need to determine the noise in the cold state. The test data were processed to obtain part of the results of bench test shown in Figure 4 (the braking pressure is 2.0 MPa, and the rotational speed is 120 rpm), which is representative. Table 2 shows the noise occurrence rate at different frequency bands. The row data in the table indicate the occurrence rate of noise under each frequency band at the same sound pressure level, and the column data indicate the occurrence rate of noise under

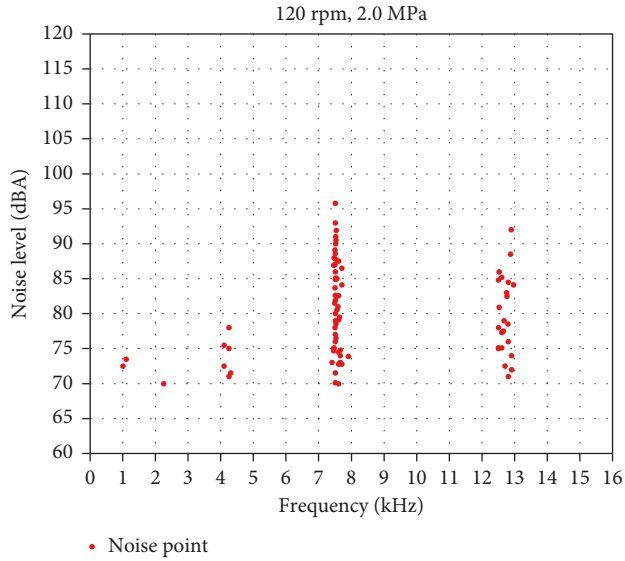

Figure 4: Noise frequency distribution and sound pressure level.

Table 2: Noise occurrence rate at different frequency bands.

Brake application: 1,430	Number	Rate (%)	f_1 (%) Near 7.5 kHz	f_2 (%) Near 12.7 kHz	f_3 (%) Near 4.1 kHz	f_4 (%) Near 1.0 kHz	f_5 (%) Near 2.2 kHz
Total noisy brake	325	22.73	10.98	8.18	2.17	1.12	0.28
70–80 dBA	141	9.86	3.71	2.73	2.03	0.28	0.28
80–90 dBA	129	9.02	5.03	3.85	0.14	0.00	0.00
90–100 dBA	46	3.22	1.89	1.33	0.00	0.00	0.00
100–110 dBA	9	0.63	0.35	0.28	0.00	0.00	0.00
110–120 dBA	0	0.00	0.00	0.00	0.00	0.00	0.00
>120 dBA	0	0.00	0.00	0.00	0.00	0.00	0.00

Table 3: Comparison between the results of complex eigenvalue analysis and the bench test of brake squeal.

Simulation conditions		The central frequency of squeal (Hz)					
n = 120 rpm	Test results	—	—	7,561.6	—	12,737.1	—
P = 1.5 MPa	Simulation results	5,954.7	6,404.4	7,598.4	10,360.1	12,804.0	13,969.2
μ = 0.8	Error (%)	—	—	0.49	—	0.53	—
n = 120 rpm	Test results	—	7,561.6	—	12,737.1	—	—
P = 2.0 MPa	Simulation results	6,301.6	7,571.9	10,892.0	12,752.6	—	—
μ = 0.7	Error (%)	—	0.14	—	0.12	—	—
n = 120 rpm	Test results	7,561.6	/	12,737.1	—	—	—
P = 2.5 MPa	Simulation results	7,562.7	11,035.2	12,832.5	—	—	—
μ = 0.6	Error (%)	0.01	—	0.75	—	—	—

each sound pressure level at the same frequency. It can be found from Figure 4 and Table 2 that there are five different frequencies of squeals in the braking process, and the frequencies of squeals are mainly distributed around 4.1 kHz, 7.5 kHz, and 12.7 kHz.

The test results at the braking pressure of 1.5 MPa, 2.0 MPa, and 2.5 MPa and fiction coefficient of 0.8, 0.7, and 0.6 were, respectively, extracted, and the test results were compared with the unstable modal frequency of brake system obtained by simulating to verify the validity and accuracy of the model, as shown in Table 3. The results show that all the brake squeal frequencies in the test can be predicted by simulation, and the error is controlled within 0.1%.

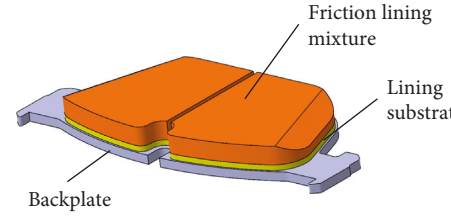

Figure 5: Composition of brake pad.

However, the phenomenon of overprediction appeared in the simulation; this is mainly due to the fact that the model of complex eigenvalue analysis does not take into account

Table 4: Material properties of each component of brake pad.

Component	Density (kg·m^{-3})	Young's modulus (MPa)	Poisson's ratio
Backplate	7,800	197,000	0.30
Lining substrate	2,800	5,350	0.35
Friction lining mixture	2,200	10,707	0.32

Table 5: Experimental verification on simulation vibration mode of the brake pad.

Order	Simulation vibration mode	Laser vibrometer
1	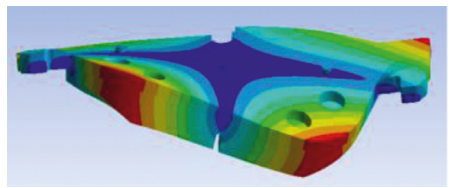	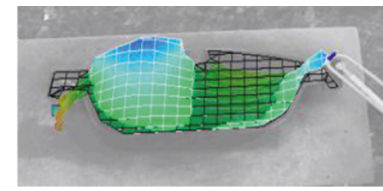
2	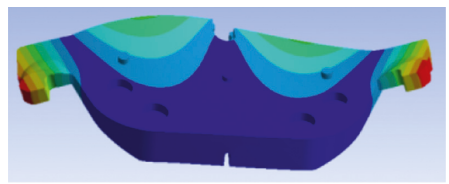	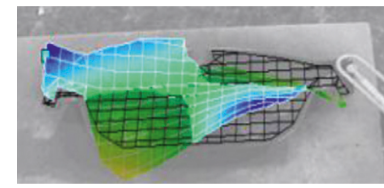
3	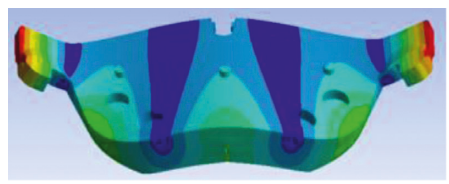	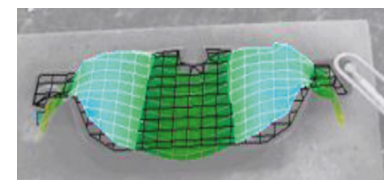
4	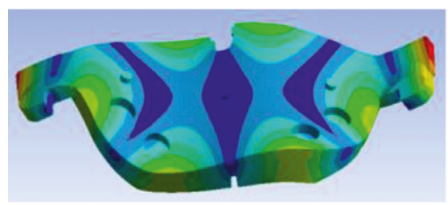	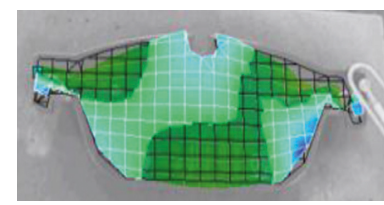
5	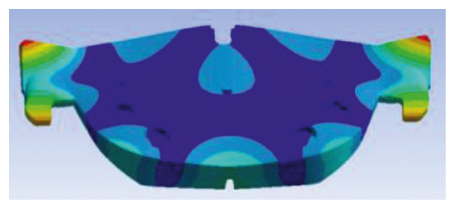	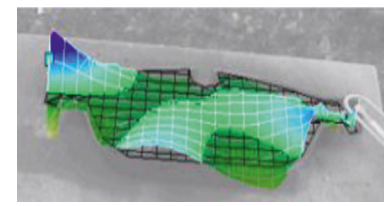

factors such as the thermomechanical coupling, the frictional characteristics, and the time-varying characteristics of material properties in the actual braking process, which is mentioned in many literatures, so the model could predict the brake squeal accurately.

4. Verification of Brake Pad

The brake pad is mainly composed of three parts, namely, backplate, lining substrate, and friction lining mixture, as shown in Figure 5. Because of the simple structure and regular shape of the brake pad, the hexahedral mesh is selected to mesh. The material properties of each component are shown in Table 4.

From the results of real modal analysis of the brake pad, the typical vibration modes of natural frequencies within 10 kHz are extracted, as shown in Table 5, which are mainly manifested as bending and torsional vibration modes. The accuracy of the natural frequency of the brake pad was verified by the FRF resonance tester. As shown in Table 6,

Table 6: Experimental verification on simulation modal frequency of the brake pad.

Simulation modal frequency		F.R.F		Error (%)
Order	Frequency (Hz)	Order	Frequency (Hz)	
1	3169	2	3151	0.57
2	4137	3	4130	0.17
3	5689	4	5610	1.41
4	7342	5	7268	1.02
5	9380	6	9395	0.16

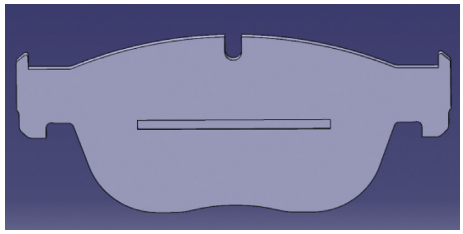

Figure 6: Sample 1 (single horizontal slot).

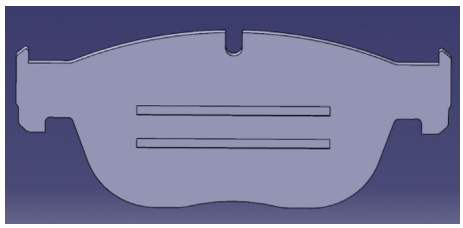

Figure 7: Sample 2 (double horizontal slots).

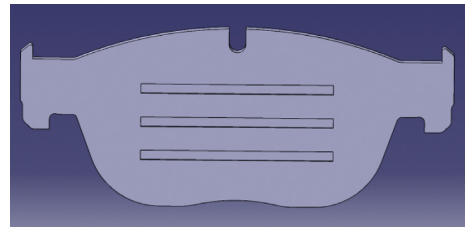

Figure 8: Sample 3 (three horizontal slots).

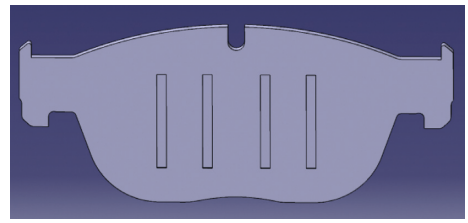

Figure 9: Sample 4 (four longitudinal slots).

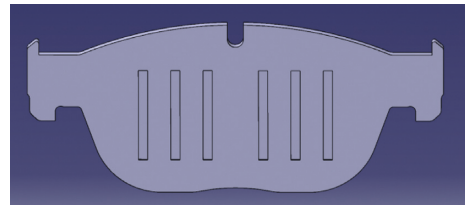

Figure 10: Sample 5 (six longitudinal slots).

the natural frequency error of the simulation and experiment was found to be within 2%. At the same time, the laser vibrometer is used to verify the vibration mode. As shown in Table 5, the typical modes measured by the laser vibrometer are exactly the same as those of the simulation vibration mode, so the results of the real modal analysis are accurate and the model of the brake pad is effective.

5. Slotting Designs on Brake Pad Backplate

According to the theory of structural dynamic design, changes in the mass of the system or the shape of the structure will lead to the change of system stiffness and damping, which will affect the natural frequency of the system [14]. According to the difficulty of backplate processing and the manufacturing process of the brake pad, five types of slotting methods are designed in this study, as shown in Figures 6–10. The effects of the five types of slotting designs on the natural frequencies and vibration modes of the brake pad are analyzed to determine whether the brake squeal noise will be further affected. The effective total area of the backplate is 4615 mm^2. The design dimension of horizontal slot is 80×4 mm, and single horizontal slot, double horizontal slots, and three horizontal slots are designed on the backplate. The ratio of the slotted area to the total area of the backplate is 6.9%, 13.9%, and 20.8%, respectively. The design dimension of longitudinal slot is 40×4 mm, and four longitudinal slots and six longitudinal slots are designed on the backplate. The ratio of the slotted area to the total area of the backplate is 13.9% and 20.8%, respectively. The depth of slotting designs is both 1 mm. In addition, the large size of the slotting on the backplate will cause the stiffness of the brake pad to drop sharply and affect the manufacturing process of the brake pad, so the ratio of the slotting area of the backplate should not be larger than 25% [15].

The free mode characteristics of the above five slotted backplates are calculated in the frequency range of 10~16 kHz. Then, the six-order critical modal frequencies were extracted and compared with the free modal frequencies of the unslotted backplate, as shown in Table 7. The bench test of the brake system has shown that the frequency of the brake squeal is mainly distributed around 4.1 kHz, 7.5 kHz, and 12.7 kHz. As can be found in Table 7, Sample 3, Sample 4, and Sample 5 are significantly improved for the critical frequency of 4.1 kHz and 7.5 kHz, but only Sample 3 has the best improvement effect on the critical frequency of 12.7 kHz, and Sample 4 and Sample 5 have barely any improvement on the critical frequency of 12.7 kHz. Therefore, Sample 3 was selected for further study.

The model of Sample 3 was made into a test piece (Figure 11), and the bench test was performed. The test results are shown in Figure 12. The test time for these tests shown in Figure 12 is close to that for those tests shown in Figure 4. Table 8 shows the main four test operations and test times of

Table 7: Comparison of critical modal frequencies between slotted backplate and unslotted backplate.

Order	Modal frequency (Hz)					
	Unslotted	Sample 1	Sample 2	Sample 3	Sample 4	Sample 5
1	3,276.5	3,257.5	3,240.8	3,214	3,208.6	3,180.3
2	4,101.7	4,064.9	4,046.2	4,010.2	4,031.2	3,997.4
3	6,660.2	6,623.6	6,589.3	6,546.7	6,580.5	6,578
4	7,379.4	7,133.6	7,045.9	6,923.6	7,039.7	6,960.4
5	12,048	12,011	12,000	11,914	11,872	11,825
6	12,891	13,060	12,585	12,121	12,776	12,711

Figure 11: Test piece of Sample 3.

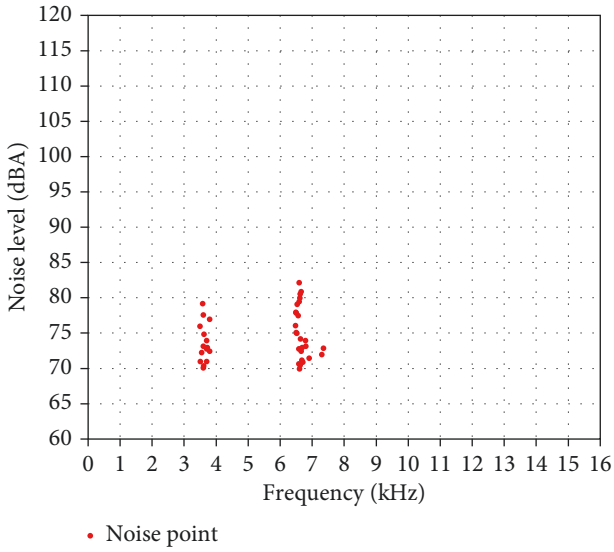

Figure 12: Noise frequency distribution and sound pressure level of the test piece.

Sample 3 which could obtain the test results shown in Figures 4 and 12. During the bench test, the braking pressure is 2 MPa and the initial rotational speed is 120 rpm.

From the test results, the brake pad with three horizontal slots on the backplate could effectively reduce the occurrence of brake squeal noise, especially that of the high-frequency squeal noise, and greatly reduce the noise points above 80 dB sound pressure level.

6. Results and Discussion

The change rate of the critical frequency between the unslotted brake pad and Sample 3 could be calculated from Table 7. The frequency changes of the Sample 3 are −91.5 Hz, −455.8 Hz, and −770 Hz, respectively, as shown in Table 9. From Figure 12, it could be found that the original squeal frequency near 7.5 kHz disappears and the new squeal noise is generated near 6.8 kHz. Similarly, the original noise frequency around 4.1 kHz disappears and the new noise is generated near 3.9 kHz. Besides, high-frequency squeal of noise points near 12.7 kHz disappears completely.

Table 8: Bench test of Sample 3.

Test operation	Snub brake	Bedding	Deceleration	Cold
Test times	40	55	45	20

Table 9: Critical frequency change rate between unslotted backplate and Sample 3.

Order	Modal frequency (Hz)		Change rate (Hz)
	Unslotted	Sample 3	
1	4,101.7	4,010.2	−91.5
2	7,379.4	6,923.6	−455.8
3	12,891	12,121	−770.0

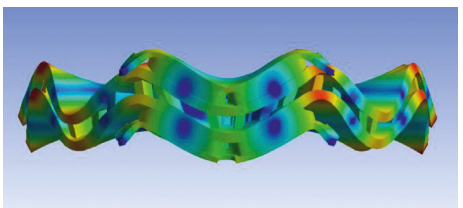

Figure 13: Unstable vibration mode at the braking pressure of 2.0 MPa (at 12,752.6 Hz).

The vibration mode of unstable modal frequency at 12,752.6 Hz is extracted from the results of complex modal analysis, as shown in Figure 13. The mode coupling between the brake pad and the brake disc resulting in resonance and the energy generated by the resonance which cannot be dissipated in time are the root causes of concentration near the high frequency 12.7 kHz. The design of three horizontal slots on the brake pad backplate makes the critical frequency change 770 Hz, which leads to the decoupling of the brake pads and the brake disc. Besides, the lining substrate of the brake pad contributes to the dissipation of energy generated by resonance. Similarly, the decoupling between the brake pads and the brake disc is also achieved at frequencies of

4.1 kHz and 7.5 kHz, but the changed brake pad modal frequencies are coupled with the other modal frequencies of the brake disc, which will easily trigger resonance and result in new noise points. At the same time, it is found that the noise distribution of the improved brake system also has a great improvement for the sound pressure level (i.e., the noise points exceeding 80 dB rarely occur). This shows that the improvement of the structure makes the noise frequencies of system near 4.1 kHz and 7.5 kHz move toward the direction of lower frequency and reduce the sound pressure level, thus achieving the effect of restraining the brake squeal noise.

7. Conclusions

(1) In this study, the design of three-layer structure of the brake pad is presented and the six-DOF kinematics model of the brake disc-brake pad is analyzed. Through the analysis of the above model, it is found that the mass and stiffness of the brake pad have an important influence on the stability of the brake system.

(2) The unstable vibration modes of the brake system are obtained from the linear complex eigenvalue analysis, and the accuracy of predictions of the complex modal analysis model is verified by the bench test of the brake system, but there is overprediction. The test results show that the noise points of the brake system are mainly distributed near the frequency of 4.1 kHz, 7.5 kHz, and 12.7 kHz.

(3) The proposed slotting design on the backplate of the brake pad by this study could greatly reduce the occurrence of brake squeal noise, especially that of the high frequency at 12.7 kHz, which provides a reliable theoretical guidance for the design of the brake system.

(4) Due to the limitation of experimental conditions, the single test object and the experimental conditions may not be comprehensive enough, so this study still has some limitations. In addition, further research is needed on how to determine the slot size and slot position accurately according to the simulation analysis and the test structure.

Conflicts of Interest

The authors declare that there are no conflicts of interest regarding the publication of this paper.

Acknowledgments

The authors acknowledge the financial support by the National Natural Science Foundation of China (51575238) and Research on key technologies of brake-by-wire system (ZY2015009).

References

[1] N. M. Kinkaid, O. M. O'Reilly, and P. Papadopoulos, "Automotive disc brake squeal," *Journal of Sound and Vibration*, vol. 267, no. 1, pp. 105–166, 2003.

[2] S. Oberst, *Analysis of Brake Squeal Noise*, Ph.D. thesis, School of Engineering and Information Technology, University College, University of New South Wales, Sydney NSW, Australia, 2011.

[3] F. Chen, "Automotive disk brake squeal: an overview," *International Journal of Vehicle Design*, vol. 51, no. 1, pp. 39–72, 2009.

[4] G. Genta and L. Morello, "The automotive chassis," *Components Design*, Springer Business Media, vol. 1, New York, NY, USA, 2009.

[5] L. Hammerstrom and S. Jacobson, "Surface modification of brake discs to reduce squeal problems," *Wear*, vol. 261, no. 1, pp. 53–57, 2006.

[6] S. Oberst and J. C. S. Lai, "Chaos in brake squeal noise," *Journal of Sound and Vibration*, vol. 330, no. 5, pp. 955–975, 2011.

[7] S. W. Kung, K. B. Dunlap, and R. S. Ballinger, "Complex eigenvalue analysis for reducing low frequency brake squeal," in *Proceedings of the SAE Technical Paper Series*, p. 109, Pittsburgh, PA, USA, March 2000.

[8] Y.-K. Hu and L. I. Nagy, "Brake squeal analysis by using nonlinear transient finite element method," in *Proceedings of the SAE Technical Paper Series*, pp. 1–8, Washingdon, DC, USA, August 1997.

[9] A. R. AbuBakar and H. J. Ouyang, "Complex eigenvalue analysis and dynamic transient analysis in predicting disc brake squeal," *International Journal of Vehicle Noise and Vibrations*, vol. 2, no. 2, pp. 143–155, 2006.

[10] Z. Zhang, S. Oberst, and J. S. C. Lai, "On the potential of uncertainty analysis for prediction of brake squeal propensity," *Journal of Sound and Vibration*, vol. 377, pp. 123–132, 2016.

[11] H. Festjens, C. Gaël, R. Franck et al., "Effectiveness of multilayer viscoelastic insulators to prevent occurrences of brake squeal: a numerical study," *Applied Acoustics*, vol. 73, no. 11, pp. 1121–1128, 2012.

[12] G. Ruhai, D. Shi, and G. A. Yao, "A research on the effects of viscoelastic ingredients in friction material formulation on the damping characteristics of brake pad," *Automotive Engineering*, vol. 30, no. 7, pp. 608–612, 2008, in Chinese.

[13] The SAE Dynamometer Test Code Committee, *Disk Brake Dynamometer Squeal Noise Matrix, SAE J2521*, SAE, Washington, DC, USA, 2013.

[14] Y. Dai, *Structural Dynamic Optimization of Vehicle Brake Pad Design for Squeal Noise Reduction*, The University of Alabama, Tuscaloosa, AL, USA, 2002.

[15] F. Massi, Y. Berthier, and L. Baillet, "Contact surface topography and system dynamics of brake squeal," *Wear*, vol. 265, no. 11-12, pp. 1784–1792, 2008.